Chapter 11

Applications of Molecular Spectroscopic Methods to the Elucidation of Lignin Structure

Tingting You and Feng Xu

Additional information is available at the end of the chapter

http://dx.doi.org/10.5772/64581

Abstract

Lignin in plant cell wall is a complex amorphous polymer and is biosynthesized mainly from three aromatic alcohols, namely, *p*-coumaryl, coniferyl, and sinapyl alcohols. This biosynthesis process consists of mainly radical coupling reactions and creates a unique lignin polymer in each plant species. Generally, lignin mainly consists of *p*-hydroxyphenyl (H), guaiacyl (G), and syringyl (S) units and is linked by several types of carbon-carbon (β-β, β-5, β-1, and 5–5) and ether bonds. Due to the structural complexity, various molecular spectroscopic methods have been applied to unravel the aromatic units and different interunit linkages in lignin from different plant species. This chapter is focused on the application of ultraviolet (UV) spectroscopy, Fourier transform infrared (FT-IR) spectroscopy, Fourier transform Raman (FT-Raman) spectroscopy, fluorescence spectroscopy, and nuclear magnetic resonance (NMR) spectroscopy to lignin structural elucidation.

Keywords: lignin, structure elucidation, 2D HSQC NMR, composition, linkages

1. Introduction

Plant cell walls in higher plants are mainly consisted of cellulose, hemicelluloses, and lignin. As a major cell wall component, lignin in plants provides rigidity, internal transport of water and nutrients, and protection against attack by microorganisms [1]. It has been reported that lignin in lignified plants accounts for 16–36% by weight [2]. Due to the high content and complex structure, lignin plays a key role in pulping and other chemical conversion process of plants. Most importantly, lignin currently attracts widespread attention as a feedstock for biofuels and

biochemical production [3–5]. Broadening the knowledge of structural features of lignin is therefore necessary to help to effectively improve the economics of these processes.

1.1. Lignin structure

Lignin is the most abundant renewable aromatic biopolymer present in nature. To the best of current knowledge, lignin shows a heterogeneous composition and lacks a defined primary structure due to the special biosynthesis processes [6]. Lignin is generally considered to be synthesized mainly from three *p*-hydroxycinnamyl alcohols precursors, namely, *p*-coumaryl, coniferyl, and sinapyl alcohols. During the lignification process, each of these precursors gives rise to a different type of lignin unit called *p*-hydroxyphenyl (H), guaiacyl (G), and syringyl (S) units, respectively. This biosynthesis process consists of mainly radical coupling, and creates a unique lignin polymer in each plant species, even in different tissues of the same individual [7]. In general, softwood (spruce, pine, etc.) lignin consists almost entirely of G units,

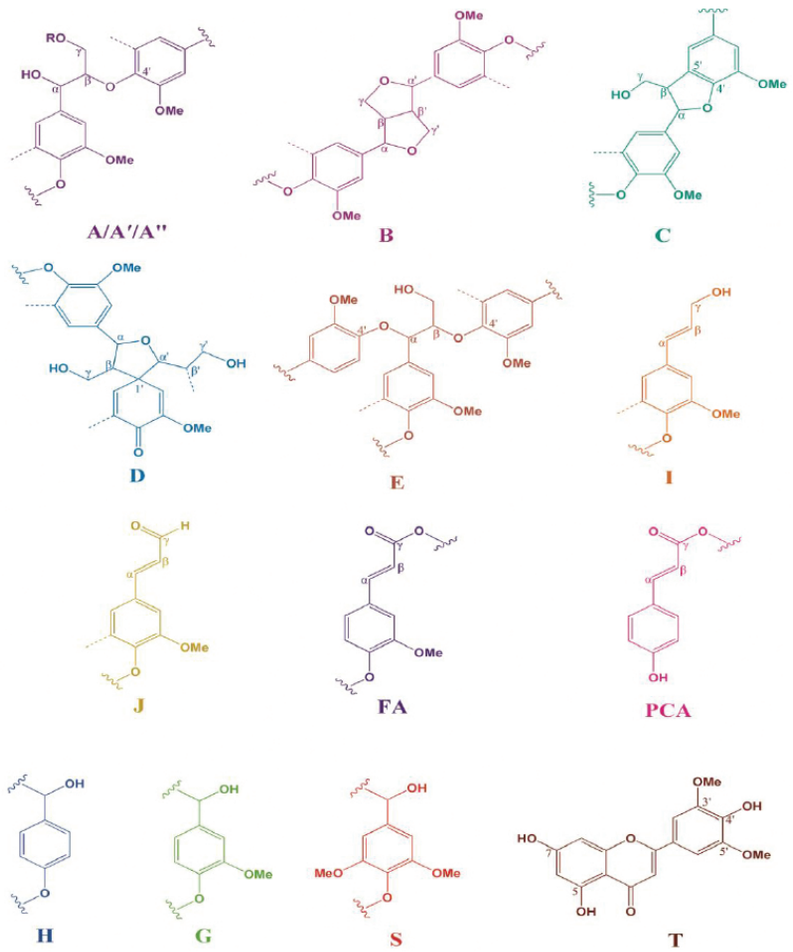

Figure 1. Main structures of lignin, involving different side-chain linkages and aromatic units: (A) β-O-4 linkages; (A′) β-O-4 linkages with acetylated γ-carbon; (A″) β-O-4 linkages with *p*-coumaroylated γ-carbon; (B) resinol structures formed by β-β, α-O-γ and γ-O-α linkages; (C) phenylcoumarance structures formed by β-5 and α-O-4 linkages; (D) spirodienone structures formed by β-1 and α-O-α linkages; (E) α, β-diaryl ether substructures; (H) *p*-hydroxyphenyl unit; (G) guaiacyl unit; (S) syringyl unit; (I) cinnamyl alcohol end-groups; (J) cinnamyl aldehyde end-groups; (FA) ferulate; (PCA) *p*-coumarate; (T) tricin.

http://dx.doi.org/10.5772/64581

hardwood (beech, poplar, etc.) lignin is a mixture of G and S units, and herbaceous lignin (bamboo, reed, etc.) is composed of all the three units. These units are linked by several types of carbon-carbon (β-β, β-5, β-1, and 5–5) and ether bonds (β-O-4 and α-O-4) with various percentage. The β-O-4 linkages are the main lignin interunit linkages, accounting for more than 60% among various linkages. However, the less C─C linkages constitute some of the most difficult bonds to break [8]. In addition to lignin, the local noncovalent interaction and oxidative reactions among carbohydrates, phenolic components, and lignin render and control the formation of lignin-carbohydrate complex (LCC) during lignin biosynthesis processes [9, 10]. Other components, such as hydroxycynnamic acids and tricin, have been demonstrated to be incorporated into herbaceous lignin, apparently making the structure of lignin more complex [7]. **Figure 1** shows the structure of main components of lignin.

1.2. Methods for structural elucidation of lignin

Lignin chemists have devoted their efforts to reveal the molecular details of lignin structure over the past few decades. Various wet-chemistry methods have been developed. Permanganate oxidation, nitrobenzene oxidation, GC-MS pyrolysis, thioacidolysis, and derivatization followed by reductive cleavage (DFRC) methods partially degrade lignin polymer and release diagnostic monomers, which reveals H/G/S composition in lignin. The presence of acylating groups in some herbaceous lignins is well known for a long time. A modified DFRC method (DFRC′) was developed for naturally acetylated lignin moieties determination [11]. Though significant strides have been made in elucidating the chemical structure of lignin by wet-chemistry methods, they have not yet been completely elucidated. Only a fraction of lignin was analyzed and significantly different results were obtained even for the same sample by different wet-chemistry methods. Moreover, all protocols provide relative comparison in an array of samples rather than giving the absolute quantitative values.

Attempts through the years have been made to develop nondestructive and quantitative methods for w using molecular spectroscopic methods. Molecular spectra see differences in chemical structure of lignin that it is invisible for other analytical methods. Acid-soluble lignin in biomass is determined to be less than 4% by ultraviolet (UV) spectroscopy based on Beer' Law. On the other hand, the level of purity originated from different resources was easily determined by comparison of the extinction coefficients [12]. Despite some constituents can also be found from the UV spectra, further evidence is needed to confirm that. To date, natural lignin is found to contain several functional groups and chromophores which can be qualitatively determined by Fourier transform infrared (FT-IR) spectroscopy, FT-Raman spectroscopy, and fluorescence spectroscopy [13–15]. FT-IR spectroscopy is the most widely distributed as a modern and powerful analytical technique. The structural changes during physical and chemical pretreatment were monitored, which revealed the mechanism [16, 17]. However, no quantitative information about both lignin interunit linkages and S/G/H composition was achieved until the application of nuclear magnetic resonance (NMR). Development of 1D, 2D, and 3D NMR spectroscopic methods provides a powerful tool for lignin analysis. Evidence of the presence of lignin substructure dibenzodioxocine and spirodienone in lignin was first observed by the NMR spectroscopic methods [18, 19]. It is noted that more detailed structure

of the whole macromolecule can be obtained by NMR spectroscopic methods. In addition to the structure details, the absolute amount of the side chain moieties and functional groups can be determined by combination of ^{13}C NMR and 2D HSQC NMR spectroscopic methods [20].

This chapter describes the application of UV spectroscopy, fluorescence spectroscopy, FT-IR spectroscopy, FT-Raman spectroscopy, and various one-dimensional and multidimensional NMR spectroscopic methods in lignin structure determination.

2. UV spectroscopy

Ultraviolet spectroscopy has been widely applied to quantitatively measure the acid-soluble lignin content, semiquantitatively determining the lignin purity, and predicting the possible lignin constituents [21–23]. The location of maximum absorption and the extinction coefficient of it are the two main factors that determine the properties of lignin.

Capitalizing on the stronger absorbance of lignin compare with carbohydrates in the UV region, the amount of acid-soluble lignin can be determined by applying Beer' Law. In 1985, a standard protocol was developed by the Technical Association of the Pulp and Paper Industry (TAPPI) to determine the amount of acid-soluble lignin and was applied widely across the world [24–26]. However, the accuracy is affected by measuring the absorbance at 200–205 nm, where carbohydrate monomers may also absorb light. Moreover, the extinction coefficient that is used varied with the type of lignin. In 2008, more accurate method of laboratory analytical procedure (LAP) of biomass was provided by the National Renewable Energy Laboratory (NREL) [27]. For the measurement, the absorbance of ASL was recorded at the recommended wavelength, which varied among plant species. Nowadays, many scientists use LAP for the determination of ASL in untreated and pretreated biomass. Our previous research applied LAP procedure to determine the content of ASL before and after ionic liquid-acid pretreatment, and an increased ASL was found [17]. Likewise, Rajan et al. used NREL methods to reveal the effect of dilute acid pretreatment on ASL of wheat straw [28].

Generally, the UV spectrum of lignin exhibits several absorption maxima at around wavelengths of 200, 240, 280, and 320 nm, which originate from the intrinsic structure [29]. Occurrence of the maximum absorption at around 200 nm in UV spectra is corresponding to the $\pi \rightarrow \pi^*$ electronic transition in the aromatic ring of lignin structure. Maxima at around 240 and 282 nm probably originate from the free and etherified hydroxyl groups. Phenolic structure and phenylpropane units (S, G) in lignin also can be detected from the UV spectra [22, 30]. It is reported that a pure syringyl lignin has an absorption maximum at 270–273 nm, whereas a red shift to 280–282 nm and three times stronger extinction coefficient are found in a pure guaiacyl lignin [22]. As for the maximum absorption at around 320 nm, it is attributed to $\pi \rightarrow \pi^*$ transitions in lignin units with $C_\alpha{=}C_\beta$ linkages conjugated with aromatic ring and $n \rightarrow \pi^*$ transition in lignin units containing $C_\alpha{=}O$ groups. In herbaceous plants, bound hydroxycinnamic acid especially a predominance of esterified *p*-coumaric acid or etherified ferulic acid may contribute to the appearance of it [7, 31].

http://dx.doi.org/10.5772/64581

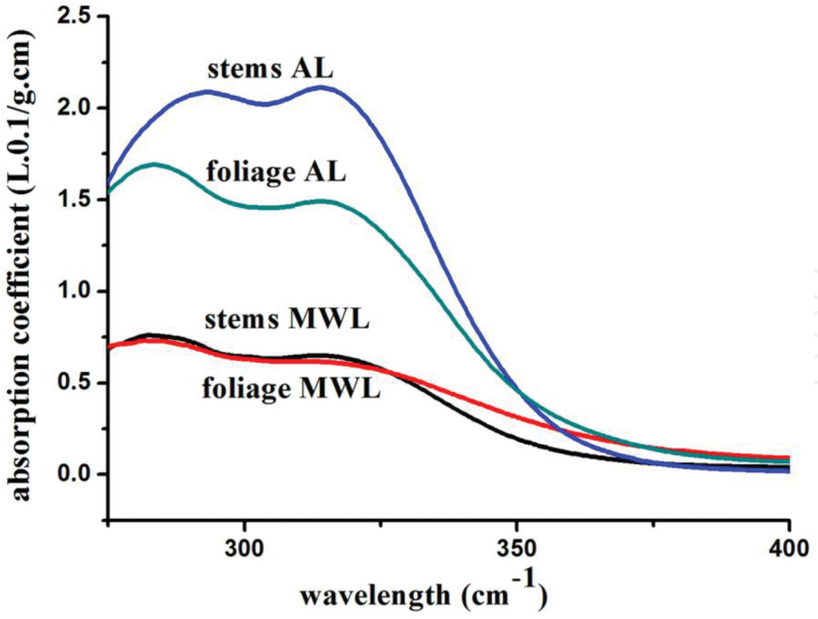

Figure 2. UV spectra of stem milled wood lignin (MWL), foliage MWL, stem alkaline lignin (AL), and foliage AL from *A. donax*. The lignin fractions were dissolved in DMSO, and scanned from 500 to 190 nm on a UV 2300 spectrophotometer (reprinted with permission from [7]. Copyright 2013 American Chemical Society).

The UV spectroscopic patterns of lignin cary among plant species. It has been demonstrated that the maximum of the absorption curve of milled wood lignin (MWL) from spruce fibers is at about 280 nm, whereas the UV spectra of acid insoluble lignin fractions from shrubs *Caligonum monogoliacum* and *Tamarix* spp. exhibits two absorption maxima at around 245 and 280 nm [22, 32]. It is noted the UV spectra of grasses are somewhat different from wood species. Apart from the first maximum absorption at 284 nm, a shoulder peak at around 320 nm is always appeared in the UV spectrum of lignin from grasses [7, 33]. For instance, esterified *p*-coumaric acid is the main component if the wavelength of maximum absorption is shorter than 320 nm. In contrast, the wavelength of maximum absorption at 325 nm is indicative of rich etherified ferulic acid in lignin. **Figure 2** shows UV absorption spectra of stem MWL, foliage MWL, stem alkaline lignin (AL), and foliage AL from energy crops *Arundo donax* Linn. that reprinted from our previous article [7]. As illustrated, two maximum absorptions were found at around 284 and 310 nm in the spectra of lignin fractions. It can be inferred that the four lignin fractions may contain free and etherified hydroxyl groups, and bound *p*-coumaric acid.

UV spectroscopy has been used to semiquantitatively determine the purity of lignin with respect to the concentration. According to Beer's Law ($A = \varepsilon cd$, where A = absorbance, ε = extinction coefficient, d = path length, c = concentration), the value of extinction coefficient reveals the concentration of lignin. The low extinction coefficient of lignin is due to the high amount of nonlignin materials. As aforementioned, lignin in plant tissue does not exist as an independent polymer but bonded with polysaccharides, which can be coextracted. The presence of a variety of variable abundances of lignin-carbohydrate bonds among different plant species makes it difficult to isolate lignin purely and completely. Sugar analysis of isolated cellulolytic enzyme lignin from Douglas fir, redwood, white fir, *Eucalyptus globulus*

Labill., *A. donax*, and poplar wood revealed that lignin contained relatively noticeable amount (7.74–20%) of associated carbohydrates [34–36], which reduces the level of purity. Moreover, lignin fractions isolated from lignocellulosic biomass still contain other nonlignin contaminants, for instance, ash. Specifically, the ash content in technical lignins such as lignosulfonate (LS) and kraft lignin (KL) is up to 9.4 and 27.1%, respectively [37]. A certain amount of ash in lignin was demonstrated to decrease the extinction coefficient. Sun et al. found that the relatively lower absorption of lignin fractions was probable due to the higher amounts of coextracted nonlignin materials such as ash and salts [21].

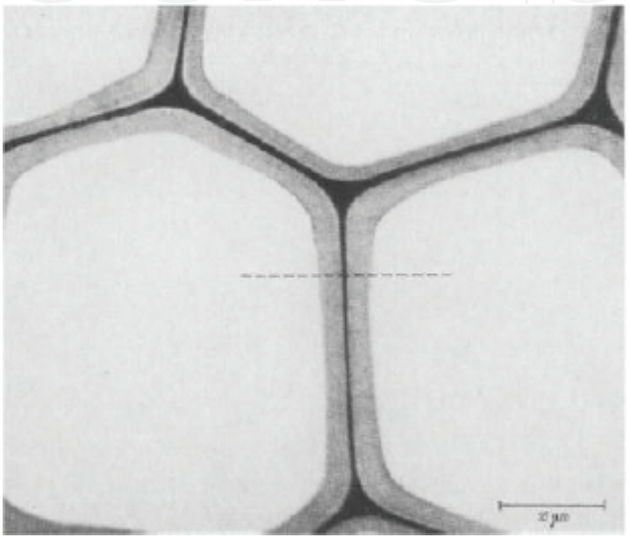

Figure 3. Cross section of Epon embedded tracheids of black spruce earlywood photographed in ultraviolet light of wavelength 240 nm. The densitometer tracing was taken across the tracheid wall on the dotted line (reprinted with permission from [38]. Copyright 1969 Springer).

Apart from UV spectroscopy, UV microscopy has been used in a number of studies to monitor the lignin distribution among various tissues of gymnosperm and dicotyledonous angiosperm in respect to the concentration by comparison of UV absorbance. UV light transmits through ultrathin sections (0.5 μm) of wood and measure within the wavelength range 240–320 nm of lignin absorption. From the absorbance and the cell wall dimensions, the concentrations of lignin in cell wall layering structure of earlywood of black spruce (**Figure 3**) are determined to decrease in the order: the cell comers > the compound middle lamella > the secondary wall [22, 38].

3. Fluorescence spectroscopy

Fluorescence spectroscopy has been used for the analysis of lignin constituents in wastewaters from pulp mills in the 1970s [14]. Subsequently, scientists focus a lot on the fluorescence properties of lignin. Lundquist et al. have investigated the fluorescence spectra of a variety of

http://dx.doi.org/10.5772/64581

model compounds, lignin, and lignin-related products to establish a basis for the interpretation of the fluorescence results [39]. By comparing the fluorescence spectra (emission spectra and excitation spectra) of lignin with the structural elements, the possible chromophores can be determined.

Dioxane-water or water is a good solvent for the dissolution of lignin as the absorbance of these solutions is less than 0.05. This implied that the intensity of the emitted light (Q) can be expressed by the following equation [39, 40]: $Q = I_0\ (2.3\varepsilon cd)\ \Phi_f$, where ($I_0$ = intensity of the incident light, ε = molar absorptivity, c = concentration in moles per liter, b = sample path length, Φ_f = quantum efficiency for fluorescence). Albinsson et al. dissolved the untreated and borohydride-reduced MWL from spruce in dioxane-water 9:1 for the fluorescence spectra collecting [14]. Lundquist et al. used either water or dioxane-water 1:1 as the solvents to explore the fluorescence properties of lignin sulfonate, MWL, and kraft lignin [39].

Sample*	Excitation spectrum λ_{max} (nm)	Emission spectrum λ_{max} (nm)
MWL from spruce [39]	285, 240	358
MWL from spruce [14]	280	364
Borohydride-reduced MWL from spruce [39]	284, 240	358
MWL from birch [39]	282, 240	350
Kraft lignin [39]	334	398
Lignin sulfonate [39]	287, 240, 315	393

Note: *Reference.

Table 1. Fluorescence properties of lignin materials.

Nonradiative energy transfer from lignin chromophores is excited to an acceptor and then emits the fluorescent light. Excitation spectra and emission spectra were collected on a spectrofluorimeter. Generally, the emission spectra are recorded at the wavelengths of the excitation maxima and the excitation spectra are recorded at the wavelengths of the emission maxima. **Table 1** shows the fluorescence properties of lignin materials [14, 39]. As can be seen, emission spectra of MWL from spruce exhibit a maximum at about 360 nm on excitation at different wavelengths in the range 240–320 nm. For the MWL from birch, emission spectra exhibit a maximum at 350 nm. A great difference is found for the fluorescence properties of technical lignin, such as kraft lignin or lignin sulfonate. The emission spectra of these lignins exhibit a maximum at about 400 nm on excitation at different wavelengths in the range 240–350 nm.

Examination of the fluorescence spectra of lignin samples and model compounds suggested the possible chromophores. If the structural elements spectra closely match the emission from the lignins, it points to the possibility that the lignin fluorescence is mainly emitted from that structure of lignin. Based on these, small amounts of phenylcoumarone structures are found in lignin from pretreated acid or balling materials [14]. Reduction of carbonyl in lignin by

borohydride does not change the position of emission maximum but increase the fluorescence intensity due to some "energy sink" structure in lignin. It has been determined that the "energy sink" structure could be arylconjugated carbonyl groups such as cinnamyl alcohol or phenylcoumarone type and stilbene structure.

Lignocellulosic biomass is known to be autofluorescent. Compared with holocellulose, the autofluorescent of lignin is generally much brighter [41, 42]. Laser scanning confocal fluorescence microscopy (LSCFM) allowed direct visualization of the relative amounts of lignin in different cell types on a semiquantitative basis. Based on the brightness of fluorescence images, the relative amounts of lignin in different regions of the cell wall in different cell types can be measured [43]. Donaldson et al. used confocal fluorescence microscopy (FM) to provide semiquantitative information in different regions based on lignin autofluorescence, and by staining with acriflavine [44]. The level of lignification in different plant species was then determined. FM was also used to investigate the cell wall structure changes during chemical pretreatment of biomass [45].

4. FT-IR and FR-Raman spectroscopy

Fourier transform infrared and FT-Raman spectroscopic methods have been described as an efficient measurement of valuable plant components, such as lipids, fatty acids, carbohydrates, phenolic substances, and so forth [46]. Results from both FT-IR and FT-Raman spectroscopy are in general agreement and provide complimentary information. Both techniques are nondestructive, rapid, and accurate and use only microscale samples. Differed from FT-IR spectroscopy, FT-Raman spectroscopy is insensitive to water. Hence, it is more suitable to perform in situ studies of fresh plant materials that contained some moisture by FT-Raman spectroscopy. The application of these two techniques to numerous research areas has already provided useful information on lignin.

4.1. FT-IR spectroscopy

FT-IR spectroscopy is a nondestructive, noninvasive, high sensitivity, and rapid method for lignin structure investigation or wood constituent determination widely use by lignin and wood chemists as a molecular probe [13, 47, 48]. This method opens perspective to quantify lignin in samples and semiquantitative and qualitative analyses of lignin structure characteristic.

4.1.1. FT-IR spectra assignment

Much work has been published on the characterization of lignin, and a lignin FT-IR-spectrum library has been established over the past few decades. Transmission or diffuse reflectance spectra in the midinfrared (4000–200 cm^{-1}) have been shown to provide reliable information on the chemical properties of lignin fractions or lignin in wood. Before the analysis, all of the spectra should be baseline corrected and normalized. In the region 3800–2750 cm^{-1}, several bands are observed which are caused by the presence of alcoholic and phenolic hydroxyl

http://dx.doi.org/10.5772/64581

groups and the methyl and methylene groups in lignin [47]. More bands are clearly discernible with deconvolution. In more detail, a wide absorption band appearing at 3580–3550 cm^{-1} is derived from free hydroxyl group in phenolic and alcoholic structures. Additionally, signals in the region 3000–2750 cm^{-1} are predominantly arising from C-H stretching in aromatic methoxyl groups and in methyl and methylene groups of the side chain. Fatty acid present in lignin undoubtedly increases the intensity of C-H stretching [49]. Demethylation or methylation affects the intensity of these bands sharply. It has been reported that the intensity of O-H stretching peak reduces dramatically upon methylation, whereas the intensity of peaks corresponding to C-H stretching increased simultaneously [50].

The investigation of more complex fingerprint region is necessary to facilitate understanding of the intact lignin characteristics. Bands found at around 1735 and 1714 cm^{-1} are originated from unconjugated carbonyl-carboxyl stretching in ketones, carbonyls, and ester groups [13]. Esterified phenolic acids and acetyls from associated hemicelluloses are the contributors to these absorption bands. The intensity of these bands also increased when a ketone or an aldehyde structure is produced [51]. However, the occurrence of a serial of absorption peaks at range 1675–1655 cm^{-1} is corresponding to conjugated carbonyl-carboxyl stretching. Hergert et al. concluded that the peak at 1660 cm^{-1} was originated from a ketone group located at α position, whereas the peak at 1712 cm^{-1} was assigned to a ketone group located at β position [52]. It is noteworthy that sharp bands at 1653 cm^{-1} from the spectrum of oven-dried samples are probably arising from the tricin associated with lignin especially from nonwood biomass [7, 25, 53].

Every lignin FT-IR spectrum shows prominent absorptions at around 1600, 1510, and 1420 cm^{-1} and the C—H deformation combined with aromatic ring vibration at 1460 cm^{-1}. The first three bands are assigned to the aromatic skeleton vibrations in lignin, which is the "core" structure of lignin. According to the classification of lignin proposed by Faix, the FT-IR spectra of lignin are divided into three categories, i.e., G type, GS type, and GSH type [13]. The spectra of type G lignins show typical feature at 1140 cm^{-1}, which originates from aromatic C—H in-plane deformation. Structure features of G type lignin are primary found in the spectrum of softwood lignin. Generally, the spectra of lignin samples from softwood, such as pine and spruce, show absorptions at 1269 cm^{-1} (G ring and C═O stretch), 1140, 854, and 817 cm^{-1} (C—H out-of-plane vibrations at positions 2, 5, and 6 of G units). Lignin from hardwood such as poplar, birch, and beech belongs to GS type according to the IR classification criteria [13]. GS type lignin exhibites typical features at a wavenumber at around 1128 (aromatic C—H in-plane deformation), 1328 (S ring plus G ring condensed), and 834 cm^{-1} (C—H out-of-plane in position 2 and 6 of S). Furthermore, the spectra within the GS category are subdivided into four groups based on different intensities of each band. In the samples from *A. donax* and bamboo, the absorption band at 1167 cm^{-1} which is attributed to C═O in ester groups (conjugated) is additionally present compared to the spectra of GS and G type lignin [7, 54]. Hence, maxima absorption at 1167 cm^{-1} is typical only for GSH type lignin. Signals from lignin functional groups such as phenolic hydroxyl group can be found at 1370–1375 cm^{-1}. As small amount of carbohydrate is apt to associate with lignin, aromatic C—H deformation at 1035 cm^{-1} appears as a complex vibration associated with the C—O, C—C stretching and C—OH bending in polysaccharides. For more details, see **Table 2** [7, 13, 47, 55].

Frequency (cm^{-1})	Assignment	Comments
3000–2840	ν (C—H)	C—H stretching vibrations in methyl and methylene of side chains
1738–1709	ν (C═O)	C═O stretching in unconjugated ketone, carbonyl and ester; C═O stretching in conjugated aldehydes and carboxylic acids absorb around and below 1700 cm^{-1}
1699–1633	ν (C═O)	C═O stretching in conjugated aldehydes and carboxylic acids absorb around and below 1700 cm^{-1}
1684	ν (C═O)	*β*-enone carbonyl stretching modes
1655–1675	ν (C═O)	C═O stretching in conjugated para-substitute aryl ketones
1593–1605	ν (Ar), ν(C═O)	Aromatic skeletal vibrations of S and G (S > G) plus C═O Stretching; S > G and G Condensed > G etherified
1510	ν (Ar)	aromatic skeletal vibrations of S and G (G > S)
1460	ν (C—H)	Asymmetric C—H deformations in —CH_3 and —CH_2
1420	ν (Ar)	Aromatic skeletal vibrations combined with C—H in-plane deform
1365–1370	ν (C—H), ν (O—H)	Aliphatic C—H stretching in CH_3 and phenolic OH
1267	ν (Ar), ν(C═O)	G ring and C═O stretching
1221–1230	ν (C═O), ν (C—O), ν (C—C)	C—C, C—O and C═O stretching (G condensed > G etherified)
1167	ν (C═O)	Typical for HGS type lignin; C═O stretching inconjugated ketone, ester groups
1124	δ (C—H)	Aromatic C—H bending in-plane (typical for S units)
1030–1035	ν (C—H)	The aromatic C—H deformation acting as a complex vibration associated with the C—O, C—C stretching and C—OH bending
966–990	ν (—HC═CH—)	—HC═CH- out-of-plane deformation (trans)
853–858	ν (C—H)	C—H out of plane in position 2, 5, and 6 of G units
834	ν (C—H)	C—H out of plane in position 2 and 6 of S units, and in all positions of H units

Table 2. Main assignments of lignin in FT-IR bands.

4.1.2. Qualitative and semiquantitative analysis

FT-IR spectroscopy reflects the chemical structure of lignin. As a result, the native characteristics are uncovered and the structural changes taking place in samples are monitored. Huang et al. found that some tannin was possibly condensed with bark lignin by comparing with the FT-IR spectra discrepancy of MWLs from loblolly pine stem wood, residue, and bark [26]. Moreover, all of the three MWLs belonged to G type lignin. Differed from the softwood lignin, MWL from energy crops *A. donax* showed features of GSH type lignin. A treatment is involved in efficient utilization of lignocellulosic biomass. It is demonstrated that the "core" structure of lignin samples isolated by alkaline, ionic liquid, organic solvents, acid, and thermal treatment does not change significantly. However, the absorption frequencies correspond to

http://dx.doi.org/10.5772/64581

the vibrational motions of the nuclei of a functional group show distinct changes when the chemical environment of the functional group is modified. Jia et al. found that a ketone structure was produced during acidic ionic liquid treatment of lignin model compound by comparing the FT-IR spectra that resulted from the cleavage of β-O-4 linkage [51]. Chen et al. have reported that the shift of 1505–1510 cm^{-1} accompanied with the increased intensity of the band at 1321 cm^{-1} identified by attenuated total reflectance (ATR)-FTIR spectra of lignin indicated the occurrence of condensed reaction during the heat treatment [56]. It should be noted that the ATR-FTIR only quantitatively determined the chemical changes in the surface of the samples. Further evidence was needed to confirm that.

Apart from the qualitative analysis, FT-IR spectroscopy has been utilized as a means of relative quantifying lignin in samples. Raiskila et al. have developed a method based on the FT-IR spectra to determine the relative amount of lignin in a large amount of samples [57]. In addition to the lignin content determination, the condensation indices (i.e., the cross-linking indexes) of lignin reflect the condensation degree of lignin, which can be expressed by the following formula [58, 59]:

$$\mathrm{CI} = \frac{\text{Sum of all minima between 1500 and 1050 cm}^{-1}}{\text{Sum of all mixima between 1600 and 1030 cm}^{-1}}$$

Lignin condensation always occurred during the acid treatment or the severe ball milling. The quantitatively analysis of the CI by using FT-IR spectroscopy is extremely convenient and time saving. Furthermore, the Abs. 1742/Abs. 1768 ratio is positive in connection with the phenolic hydroxyl group in lignin [60].

4.2. FT-Raman spectroscopy

1064 nm excited FT-Raman spectroscopy overcomes the obstacle of lignin autofluorescence, and the Raman spectra of acceptable quality for lignin or lignin-related materials can be obtained. Compared with the FT-IR spectra, more bands can be detected in the FT-Raman spectra. It has been reported that in neat state only about 60% of the bands of the total detected FT-Raman bands are detected in the FT-Raman spectra, implying that 40% of the bands could only be detected by FT-Raman [62]. In addition, fresh plants even with some extract present in them do not affect the FT-Raman spectral data. It is therefore significant to use both Raman and IR analyses to obtain the most detailed chemical information of lignin.

4.2.1. FT-Raman spectra assignment

The band assignment information in a lignin FT-Raman spectrum has been achieved primarily by Agarwal and his group [15, 61–64]. In general, the spectra are divided into three regions: 3200–2700, 1850–1350, and 1450–250 cm^{-1} region. In the region 3200–2700 cm^{-1}, several bands derived from the aliphatic and aromatic C─H stretches are detected. By studying the spectra of benzene derivatives and lignin models, it is determined that band at around 3070 cm^{-1} is likely to be due to the aromatic C─H stretch. The bands at approximately

3007 and 2938 cm^{-1} are originated from the asymmetric aliphatic C—H stretch like methoxy and acetoxy groups, whereas the band at 2843 cm^{-1} can be assigned to the symmetric aliphatic C—H stretch. A high amount of S units and acetylation or methylation treatments give particularly more intense 2938 cm^{-1} band [15]. Another band at 2890 cm^{-1} is assigned to the C—H stretch in R_3C—H structures.

The 1850–1350 cm^{-1} region is the most informative region for lignin. This region contains bands due to aromatic rings, ring-conjugated ethylenic C=C, α- and γ-C=O, and the *o*- and *p*-quinones. Every FT-Raman spectrum of lignin exhibited a strong band at about 1600 cm^{-1}, and can be used to normalize the spectra. This band is due to the aromatic ring stretch, and the band intensity is enhanced by the conjugation and resonance Raman effect [62]. Nonsymmetrical shape of the band suggested that two more components are included. After curve-fit treatment of the band of lignin from hardwood samples, S-marker and G-maker bands occurred. The calculation of these two bands would be a good probe to quantify the S/G ratio [65]. The band at 1660 cm^{-1} is assigned to ethylenic C=C bond in coniferyl alcohol units and the γ-C=O in coniferaldehyde units in lignin, whereas the band at 1630 cm^{-1} is found to be associated with the ring-conjugated C=C bond in coniferaldehyde units.

The 1450–250 cm^{-1} region reveals more details of lignin substructures. FT-Raman study of a large number of dehydrogenation polymer (DHP) lignin and hydroxycinnamic acid standard compounds is essential to establish a basis for the interpretation of FT-Raman spectra for lignin. Agarwal et al. collected and compared the spectra of G-DHP, S-DHP, and H-DHP lignin [63]. It was demonstrated that the bands at 371, 1041, 1333, and 1456 cm^{-1} were mainly resulted from the S type lignin, whereas the band at 1271 cm^{-1} was originated from G type lignin. Further investigation of softwood and hardwood MWLs confirmed these assignments. After a preliminary study of the spectra of hydroxycinnamic acid standard compounds and lignin, we recently showed that the band at 1173 cm^{-1} was assigned to C=O vibration form esterified or free hydroxycinnamic acid from grass *A. donax* [66]. A similar band at around 1173 cm^{-1} was also found in the spectra of switchgrass. Another band at about 1202 cm^{-1} is attributed to ring deformation and aryl-OCH_3 and aryl-OH in-plane bending from H type lignin [67].

4.2.2. Qualitative and semiquantitative analysis

Similar to FT-IR spectroscopy, FT-Raman spectroscopy is useful to the rapid characterization of lignin. The basic lignin units and functional groups in different lignocellulosic biomass are easy to identify from the FT-Raman spectra according to the bands assignments aforementioned. Raman spectral changes show the modification of lignin aroused by chemical, mechanical, or biological treatment [15, 64]. The spectral data changes of lignin treated by acetylation, methylation, diimide treatment, and alkaline hydrogen peroxide bleaching are achieved [15].

Some of the bands in the Raman spectra are applied to quantify lignin content or lignin structure. It is interesting to found that the intensity (peak area) of band at 1600 cm^{-1} of lignin is linearly related to the kappa number of pulp (R^2 = 0.98). The residual lignin content in bleaching pulp is therefore obtained by calculating the peak area of band at 1600 cm^{-1}. It is well known that significant variation in the S/G ratio exists among different plant species. A spectral

http://dx.doi.org/10.5772/64581

deconvolution method based on FT-Raman spectroscopy holds significant promise in the rapid and accurate determination of S/G ratio quantitatively [65].

5. NMR spectroscopy

The structure of lignin macromolecule in plants is extreme complex. To investigate the structure of the whole lignin macromolecule, various nuclear magnetic resonance spectroscopic methods (one-dimensional and multidimensional NMR) in both solid and solution states are frequently utilized. Compare with other spectroscopic methods mentioned above, NMR spectroscopic methods have much higher resolution and enable a larger amount of information to be obtained. Solid-state ^{13}C cross-polarization magic angle spinning (CPMAS) NMR spectroscopy allows the investigation of lignin structure in the native state and simultaneously avoids the chemical modification for sample preparation [68]. It is suitable for the analysis of lignin samples that have restricted solubility. However, due to the low resolution, only some structural features of lignin can be observed. Despite some improvements for the solid-state NMR have been made, it is still not routinely used. Solution-state NMR spectroscopy is more powerful in lignin structural elucidation. In solution, a much better resolution is obtained and a more detailed characterization of lignin aromatic and side chain is possible. Moreover, absolute quantification or relative quantification of each substructures and linkages can be unambiguously achieved [69–71]. One of the major factors that impede the application of solution-state NMR is the difficulty in dissolving lignin. In order to enhance the solubility, lignin is subjected to acetylation by anhydride/pyridine solution before the solution-state NMR spectra collection [72]. Briefly, 100 mg of lignin is dissolved in 4 mL of a solution of acetic anhydride: pyridine (1:1). After stirring for 24 h at room temperature under the exclusion of sunlight, the mixture is concentrated under reduced pressure. Then the mixture is dropped slowly into 200 mL of ice water (pH = 2.0) to induce precipitation, and the precipitate is washed with deionized water for several time. After centrifugation and freeze-drying, acetylated lignin is obtained. It is important to note that the chemical shift of lignin moieties will somewhat shift to a higher field after acetylation [69]. Recent advances in characterization of lignin polymer by solution-state NMR methodology have been reviewed [73].

5.1. One-dimensional NMR spectroscopy

1D NMR spectroscopic methods including the solution-state ^{1}H NMR, solution- or solid-state ^{13}C NMR, and solution-state ^{31}P NMR have been utilized to routinely determine the amount of hydroxyl groups (aliphatic, phenolic, and carboxylic acid), interunit linkages, S units, G units, and H units in lignin. The databases of chemical shifts of these spectroscopies have been well established based on comparison with synthetic model compound data [74–78].

5.1.1. ^{1}H NMR spectroscopy

The ^{1}H NMR spectra of lignin can be obtained within a few minutes. **Table 3** lists the signal assignment of ^{1}H NMR data [79–82]. The integral of all signals between 6.0 and 8.0 ppm belongs

to aromatic protons in G, S, and H units, whereas those between 1.60 and 2.40 ppm and from 5.76 to 6.18 ppm are due to the hydroxyl groups in lignin. Signals derived from linkages such as β-O-4 and β-1 substructures in lignin are found in the range of 2.98–3.14 and 5.76–6.18 ppm. Moreover, signals between 4.93 and 5.09 ppm are appeared in the spectrum of lignin that contained some carbohydrates. Integration of the spectra allows the quantification of some specific moieties, such as phenolic hydroxyl groups [83].

Signal (ppm)	Assignment
9.9–9.7	Aldehyde protons from cinnamaldehyde and benzaldehyde
7.15–6.75	Aromatic protons from G
6.75–6.25	Aromatic protons from S
6.18–5.76	Benzylic OH from β-O-4 and β-1
5.09–4.93	Protons from carbohydrates
4.00–3.33	Protons from methoxyl
3.14–2.98	H_β from β-1
2.40–2.20	Protons from acetylated phenolic OH groups
2.20–1.60	Protons from acetylated aliphatic OH groups and 5-5

Note: *$CDCl_3$ was used as the solvent.

Table 3. Signal assignment for ^{1}H NMR spectroscopy of lignin*.

5.1.2. Quantitative ^{13}C NMR spectroscopy

Owing to the complex structure of lignin, there are many overlapping resonances on ^{1}H NMR spectra and only some of structure features are detected. The accuracy of calculation based on ^{1}H NMR spectra of lignin is relative low. To obtain the detailed molecular structures, both solid-state and solution-state ^{13}C NMR spectroscopic methods have been applied to investigate the structural difference between lignin fractions from different plant species since 1981 [68, 84–86]. In addition to ^{13}C NMR spectra, the collection of distortionless enhancement by polarization transfer (DEPT) CH (θ = 135°) spectra of lignin has been found to have a synergetic effect [33]. ^{13}C NMR spectroscopy allows the classification and quantification of lignin nondestructively. However, more than 24 h is needed to collect the quantitative ^{13}C NMR spectra. To decrease the experiment time without affecting the quality of spectra, 0.01M chromium (III) triacetylacetonate ($Cr(acac)_3$) is considered a relaxant which allows a 4-fold decrease in the experiment time. One has to take into account that the use of tetramethylsilane (TMS) as an internal reference (0.00 ppm) is significant. Additionally, it is noteworthy that differences in the location of some structures of lignin may happen due to their strong solvent dependency [19].

G units are identified by signals at 149.3 and 149.1 (C-3, G etherified), 147.8 and 147.4 (C-4, G etherified), 134.2 (C-1, G etherified), 119.0 (C-6, G), 114.8 and 114.6 (C-5, G), and 110.9 ppm

(C-2, G). The S units are verified by signals at 152.0 (C-3/C-5, S), 147.8 and 147.4 (C-3/C-5, S nonetherified), 134.2 (C-1, S etherified), and 104.1 ppm (C-2/C-6 S). The H units are detected at 127.6 (C-2/C-6, H), 115.5 (C-3/C-5, H), and 159.8 ppm (C-4, H). Signals related to lignin linkages are also present. The resonance of C-β, C-α, and C-γ in β-O-4 linkages produces signals at 85.9, 72.1, and 59.5 ppm. Signals from β-β were detected at 71.3 (C-γ) and 54.1 ppm (C-β). Other C—C linkages such as signals from β-5 and 5–5 linkages are found to be 66.2 (C-γ) and 125.9 ppm (C-5), respectively. Additionally, signals from different functional (carbonyl, carboxyl, and hydroxyl) groups are also detected. Apart from signals from lignin, the carbohydrates impurity also produce signals at 100, 72.3, and 63.4 ppm. It is noted that the ^{13}C NMR spectra of lignin is very complex and some signals can be overlapped by the impurity such as residual solvent and carbohydrates. Therefore, it is recommended that only a relative pure lignin fraction is suggested to analysis by this technique.

Estimation of lignin moieties and functional group is significant permitting more comprehensive information about the architecture and reactivity of lignin. The amount of side-chain moieties and functional groups can be estimated by integral at corresponding chemical shift in the spectra of lignin. The integral at 160–102 ppm is always set as the reference, assuming that it includes six aromatic carbons and 0.12 vinylic carbons; therefore, all moieties can be based on equivalences per aromatic ring [69]. However, signals belonging to carbon atoms of the same groups may be derived from different moieties. To calculate the amount of one of the moieties, the content of other moieties should be calculated first by other methods. For instance, signals at 50–48 ppm in the spectrum of both lignin belong to carbon atoms of phenylcoumaran and β-1 moieties [69]. Firstly, the amount of phenylcoumaran structures (0.03/Ar) was estimated from the resonance at about 87 ppm. Then, the integral at 50–48 ppm in the spectrum is calculated to be 0.05/Ar. Finally, the content of β-1 moieties can be calculated to be 0.02/Ar.

5.1.3. ^{31}P NMR spectroscopy

Phosphitylation of hydroxyl groups in lignin followed by quantitative ^{31}P NMR provides a valuable characterization tool for determination of the content of aliphatic hydroxyl groups, phenolic hydroxyl groups, and carboxyl group. Application of this method in lignin characterization has been reviewed by Pu et al [70]. ^{31}P NMR spectra of MWL derivatized with 2-chloro-4,4,5,5-tetramethyl-1,3,2-dioxaphospholane (TMDP) reproduced from our previous study are illustrated in **Figure 4**, and the signal assignments are labeled [17]. The quantitative results of these hydroxyl groups were obtained by peak integration with cyclohexanol (signals at 133.8–133.3 ppm) as internal standard (IS). Typical phosphitylating procedures are shown as follows.

Lignin sample (20 mg) was dissolved in anhydrous pyridine and deuterated chloroform (1.6:1, v/v, 500 μL) under stirring. Cyclohexanol (10.85 mg/mL, 100 μL) was added as an internal standard, followed by addition of chromium (III) acetylacetonate solution (5 mg/mL in anhydrous pyridine and deuterated chloroform 1.6:1, v/v, 100 μL) as a relaxation reagent. The mixture was reacted with TMDP (phosphitylating reagent, 100 μL) for about 10 min and placed into the NMR tube for ^{31}P NMR analysis [7, 17].

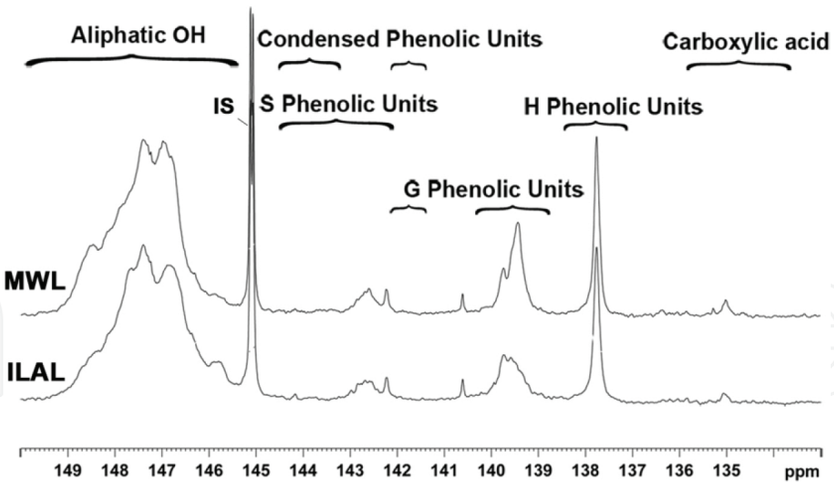

Figure 4. Quantitative ^{31}P NMR spectrum of a *A. donax* ball-milled lignin derivatized with TMDP using cyclohexanol as internal standard (reprinted with permission from [17]. Copyright 2015 American Chemical Society).

5.2. Multidimensional NMR spectroscopy

In traditional one-dimensional ^{1}H and ^{13}C NMR spectra, the signals are heavily overlapped due to the very complex and heterogeneous structure of lignin and instrumental limitations [87]. In the course of time, modern solution-state two- and three-dimensional methods are developed as efficient tools to investigate the structure of lignin. Besides better resolution, the multidimensional methods provide more reliability to the assignments [88].

5.2.1. Two-dimensional NMR spectroscopy

Two-dimensional NMR spectroscopic methods such as heteronuclear multiple quantum coherence (HMQC) spectroscopy, homonuclear Hartmann-Hahn (HOHAHA) spectroscopy, total correlation (TOCSY) spectroscopy, rotating-frame Overhauser experiment (ROESY) heteronuclear single quantum coherence NMR (HSQC) spectroscopy, and heteronuclear multiple bond coherence (HMBC) have been employed in lignin structure characterization [25, 89–91]. Among these, advanced 2D HSQC NMR is the most extensively used due to its versatility in illustrating structural features and structural transformations of isolated lignin fractions. The interpretation of 2D HSQC NMR spectra of lignin has been facilitated by the application of HOHAHA, HMQC, TOCSY, and ROESY techniques. For instance, del Río et al. performed HMBC experiment to give important information about the connectivity of the ester moiety to the lignin skeleton, and ether linkages between lignin and tricin were proposed [25]. ^{1}H-^{1}H TOCSY correlation NMR analysis can further confirm the doubted assignment of cross-peak in the spectra of HMQC or HSQC [69]. The cellulolytic enzyme lignin of *A. donax* was shown in **Figure 5**, and the main substructures are depicted in **Figure 1**.

The basic composition (S, G, and H units) and various substructures linked by ether and carbon–carbon bonds (β-O-4, β–β, β-5, etc.) can be observed in the 2D HSQC spectra (**Figure 5**). In the aromatic region (δ_C/δ_H 150–90/8.0–6.0 ppm), S, G, and H units show prominent correlations at δ_C/δ_H 103.7/6.71 ($S_{2,6}$), δ_C/δ_H 106.7/7.28 (C_α-oxidized S units S′), 110.7/6.98 (G_2),

114.9/6.72 and 6.94 (G_5), 118.7/6.77 (G_6), 127.8/7.22 ($H_{2,6}$), and 115.4/6.63 ($H_{2,6}$), respectively. It is noted that some signals may be overlapped by the others. It has been reported that signals in H units that are assigned to $C_{3,5}$-$H_{3,5}$ at δ_C/δ_H 115.4/6.63 overlapped with those from G 5-position [92]. After the alkaline treatment, intensity of signals correlated to S units is sharply increased [33]. Typically, as in spectra from grasses, prominent signals corresponding to *p*-coumarate (PCA) and ferulate (FA) structures are observed at δ_C/δ_H 115.5/6.77 ($PCA_{3,5}$), 129.9/7.46 ($PCA_{2,6}$), 111.0/7.32 (FA_2), and 111.0/7.32 (FA_6), respectively. The olefinic correlations of the cinnamyl aldehyde end-group structures (J) are observed at δ_C/δ_H 112.24/7.25 and 122.3/7.10. However, the aromatic cross-signals of the cinnamyl alcohol end-groups (I) are overlapped with the same signals in S and G units. In the side-chain region (δ_C/δ_H 90–50/6.0–2.7 ppm), cross-signals of methoxy groups (δ_C/δ_H 55.9/3.73) and β-O-4 linkages are the most predominant. The C_α─H_α correlations in the β-O-4 linkages are observed at δ_C/δ_H 72/4.7 to 4.9, while the C_β─H_β correlations are observed at δ_C/δ_H 84/4.3 and 86/4.1 for the substructures linked to the G/acylated S and S units, respectively. The C_γ-H_γ correlations in the β-O-4 substructures are found at δ_C/δ_H 60.1/3.40 and 3.72. The presence of acylating groups in some lignin produced additional intense signals. After acylation, the intense signals corresponding to acylated γ-carbon in β-O-4 substructure (A′/A″) are found in the range between δ_C/δ_H 62.7/3.83 and δ_C/δ_H 62.7/4.30. C_α─H_α correlation of carbon-carbon linkages such as resinol β-βsubstructures (B), phenylcoumaran β-5 substructures (C), spirodienone β-1 substructures (D), and α,β-diaryl ether substructures (E) are identified by the cross-peaks at δ_C/δ_H 84.8/4.66, 86.6/5.47, 81/5.01, and 79.2/5.52, respectively. In our previous research, the intensity of signals derived from β-O-4 substructures decreased during ionic liquid pretreatment suggesting the partial cleavage of this substructure [17]. With respect to signals from lignin, signals derived from carbohydrates are also found in this region and somewhat overlap with signals from C_γ-H_γ correlations in the β-O-4 substructures. For lignin-carbohydrate complex linkages investigation, the regions of δ_C/δ_H 90–105/3.9–5.4, 81.5–80/5.3–4.3, and 65–62/4.5–4.0 are of significance. Accordingly, benzyl ether LCC linkage could be detected in the region δ_C/δ_H 81.5–80/5.3–4.3; intense cross-peaks of phenol glycoside LCC linkages can be observed in the area of δ_C/δ_H 102.6–101.4/5.17–4.94, whereas cross-peaks of γ-ester linkages can be observed at δ_C/δ_H 65–62/4.5–4.0 [35, 93].

A quantitative evaluation of the lignin structure moieties has been performed successfully, and some of the quantitative methods frequently used are described. All C9 units in lignin are used as an internal standard. Integrate the G_2, $0.5S_{2,6} + G_2$, and $0.5S_{2,6} + G_2 + 0.5H_{2,6}$ signals as ISs are for softwood [91], hardwood lignin [91], and grass lignin [17, 33, 35], respectively. Based on the internal standard (all C9 units), the amount of S, G, H, and different interunit linkages could be obtained. In that way, the amount of β-O-4 linkages (% of C_9 units) was determined to be 47.0–49.4 in softwood lignin, and 60.3 in beech wood lignin, and more than 50 in grass MWL [91]. Another semiquantitative strategy of interunit linkages based on the total side chains is also acceptable for directly comparison [7, 25]. The actual extent of lignin acylation can also be estimated in the similar way particularly in grass samples [94]. In addition, Zhang and Gellerstedt proposed a quantitative method by combining ^{13}C NMR and 2D HSQC spectra, resulting in significant progress in the characterization of lignin moieties by NMR [71]. According to the method, the quantitative ^{13}C NMR spectrum was used as a reference.

Consequently, the absolute amounts of lignin substructures and even LCC moieties were quantitative calculated and expressed per 100 Ar.

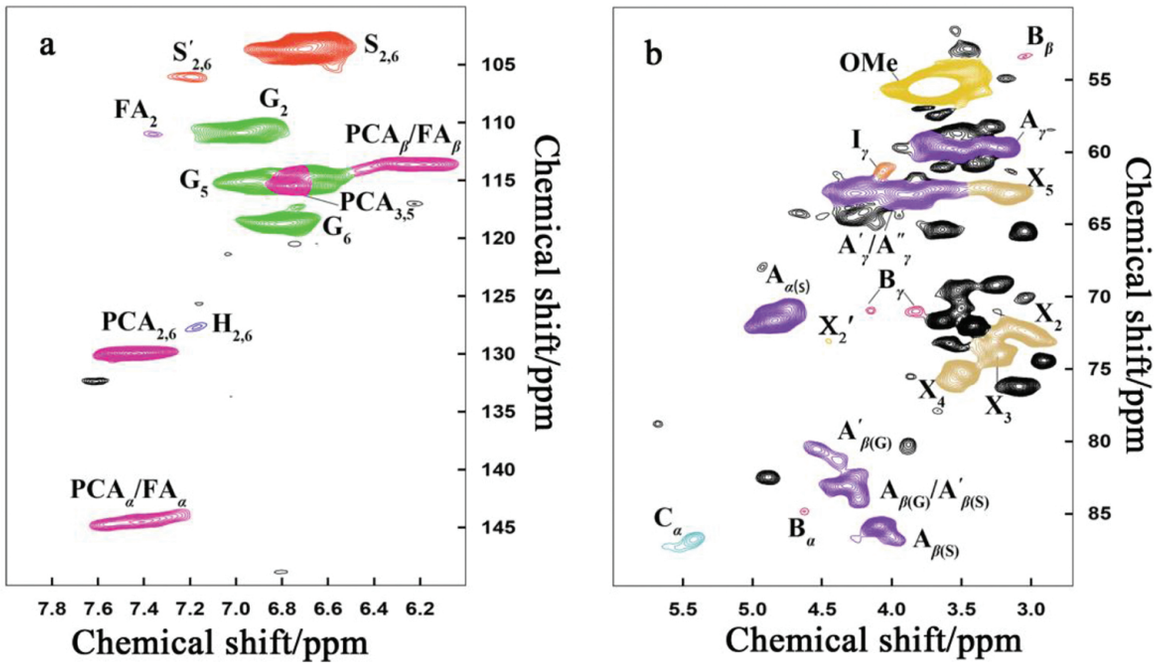

Figure 5. HSQC spectra of cellulolytic enzyme lignin from *A. donax* a aromatic region (δ_C/δ_H 150–90/8.0–6.0 ppm); b side-chain region (δ_C/δ_H 90–50/6.0–2.7 ppm). See **Figure 1** for the main lignin structures identified (reprinted with permission from [35]. Copyright 2015 Elsevier).

5.2.2. Three-dimensional NMR spectroscopy

As discussed above, the overlapping of the lignin signals cannot be fully avoided even by 2D experiments. Thanks to the rapid advances in NMR technology, the three-dimensional HSQC-TOCSY and HMQC-HOHAHA techniques are utilized to elucidate the ^{1}H-^{1}H and ^{1}H-^{13}C correlations of individual spin systems and thus indicate a certain lignin side chain structure [87, 88, 95]. The 3D spectra provide more reliability to the assignments, as the connectivity can be cross-checked from different planes of the 3D spectrum. However, long measurement time is required for the 3D experiments. As most of the structural information of lignin can be obtained by 1D and 2D NMR spectroscopic methods, the applications of 3D NMR to lignin structure characterization are still limited.

6. Conclusion and outlook

Lignin is an aromatic polymer essential for defense, water and nutrient transport, and mechanical support in vascular terrestrial plants. To reveal the molecular details of lignin structure nondestructively, various molecular spectroscopic methods have been routinely utilized. It can be inferred that the extinction coefficients of UV spectra demonstrate the purity

of lignin. Moreover, the functional groups and possible lignin composition can be obtained by the FT-IR, FT-Raman, and fluorescence spectroscopy spectral features, whereas more accurate composition and contents can be calculated using one-dimensional and multidimensional NMR spectroscopic methods. The combination of these molecular spectroscopic methods provides a comprehensive and systematic evaluation of lignin from different plant species. It was demonstrated that herbaceous plants and wood species displayed different structural characteristics of lignin, and structural modification was occurred during various treatment. Overall, these nondestructive techniques provide alternative safe, rapid, accurate, and nondestructive technology for lignin structure determination. The information of lignin presented by these molecular spectroscopic methods contributes to the understanding of native recalcitrance and facilitates the design of more effective strategies to produce lignin-based value-added materials, biochemicals, and biofules.

Acknowledgements

The authors gratefully acknowledge the financial support from National Science Foundation for Distinguished Young Scholars of China (31225005) and Chinese Ministry of Education (113014A).

Author details

Tingting You[1] and Feng Xu[1,2*]

*Address all correspondence to: xfx315@bjfu.edu.cn

1 Beijing Key Laboratory of Lignocellulosic Chemistry, Beijing Forestry University, Beijing, China

2 Key Laboratory of Pulp and Paper Science and Technology, Ministry of Education, Qilu University of Technology, Shandong, China

References

[1] Buranov AU, Mazza G. Lignin in straw of herbaceous crops. Ind Crop Prod. 2008;28(3): 237–59.

[2] Bujanovic B, Ralph S, Reiner R, Hirth K, Atalla R. Polyoxometalates in oxidative delignification of chemical pulps: effect on lignin. Materials. 2010;3(3):1888–903.

[3] Bouxin FP, McVeigh A, Tran F, Westwood NJ, Jarvis MC, Jackson SD. Catalytic depolymerisation of isolated lignins to fine chemicals using a Pt/alumina catalyst: part 1-impact of the lignin structure. Green Chem. 2015;17(2):1235–42.

[4] Xu CP, Arancon RAD, Labidi J, Luque R. Lignin depolymerisation strategies: towards valuable chemicals and fuels. Chem Soc Rev. 2014;43(22):7485–500.

[5] Laskar DD, Tucker MP, Chen XW, Helms GL, Yang B. Noble-metal catalyzed hydrodeoxygenation of biomass-derived lignin to aromatic hydrocarbons. Green Chem. 2014;16(2):897–910.

[6] Ralph J, Lundquist K, Brunow G, Lu F, Kim H, Schatz PF, et al. Lignins: natural polymers from oxidative coupling of 4-hydroxyphenyl-propanoids. Phytochem Rev. 2004;3(1–2): 29–60.

[7] You TT, Mao JZ, Yuan TQ, Wen JL, Xu F. Structural elucidation of the lignins from stems and foliage of *Arundo donax* Linn. J Agric Food Chem. 2013;61(22):5361–70.

[8] Chakar FS, Ragauskas AJ. Review of current and future softwood kraft lignin process chemistry. Ind Crop Prod. 2004;20(2):131–41.

[9] Balakshin MY, Capanema EA, Chang HM. MWL fraction with a high concentration of lignin-carbohydrate linkages: isolation and 2D NMR spectroscopic analysis. Holzforschung. 2007;61(1):1–7.

[10] Grabber JH, Ralph J, Hatfield RD. Cross-linking of maize walls by ferulate dimerization and incorporation into lignin. J Agric Food Chem. 2000;48(12): 6106–13.

[11] Ralph J, Lu F. The DFRC method for lignin analysis. 6. A simple modification for identifying natural acetates on lignins. J Agric Food Chem. 1998;46(11): 4616–9.

[12] Xu F, Sun RC, Zhai MZ, Sun JX, Jiang JX, Zhao GJ. Comparative study of three lignin fractions isolated from mild ball-milled Tamarix austromogoliac and Caragana sepium. J Appl Polym Sci. 2008;108(2):1158–68.

[13] Faix O. Classification of lignins from different botanical origins by FT-IR spectroscopy. Holzforschung-Int J Biol Chem Phys Technol Wood. 1991;45(s1):21–8.

[14] Albinsson B, Li S, Lundquist K, Stomberg R. The origin of lignin fluorescence. J Mol Struct. 1999;508(1):19–27.

[15] Agarwal UP, McSweeny JD, Ralph SA. FT-Raman investigation of milled-wood lignins: softwood, hardwood, and chemically modified black spruce lignins. J Wood Chem Technol. 2011;31(4):324–44.

[16] Sannigrahi P, Kim DH, Jung S, Ragauskas A. Pseudo-lignin and pretreatment chemistry. Energ Environ Sci. 2011;4(4):1306–10.

[17] You TT, Zhang LM, Guo SQ, Shao LP, Xu F. Unraveling the structural modifications in lignin of *Arundo donax* Linn. during acid-enhanced ionic liquid pretreatment. J Agric Food Chem. 2015;63(50):10747–56.

[18] Ralph J, Lapierre C, Lu FC, Marita JM, Pilate G, Van Doorsselaere J, et al. NMR evidence for benzodioxane structures resulting from incorporation of 5-hydroxyconiferyl alcohol into lignins of O-methyltransferase-deficient poplars. J Agric Food Chem. 2001;49(1):86–91.

[19] Zhang LM, Gellerstedt G, Ralph J, Lu FC. NMR studies on the occurrence of spirodienone structures in lignins. J Wood Chem Technol. 2006;26(1):65–79.

[20] Capanema EA, Balakshin MY, Kadla JF. A comprehensive approach for quantitative lignin characterization by NMR spectroscopy. J Agric Food Chem. 2004;52(7):1850–60.

[21] Sun R, Lu Q, Sun X. Physico-chemical and thermal characterization of lignins from Caligonum monogoliacum and Tamarix spp. Polym Degrad Stab. 2001;72(2):229–38.

[22] Adler E. Lignin chemistry—past, present and future. Wood Sci Technol. 1977;11(3):169–218.

[23] Hatfield R, Fukushima RS. Can lignin be accurately measured? Crop Sci. 2005;45(3): 832–9.

[24] TAPPI method T 222 om-83. Acid-insoluble lignin in wood and pulp. In: Test Methods 1998–1999. Atlanta: TAPPI Press; 1999.

[25] Del Río JC, Rencoret J, Prinsen P, Martínez AT, Ralph J, Gutiérrez A.. Structural characterization of wheat straw lignin as revealed by analytical pyrolysis, 2D-NMR, and reductive cleavage methods. J Agric Food Chem. 2012;60(23):5922–35.

[26] Huang F, Singh PM, Ragauskas AJ. Characterization of milled wood lignin (MWL) in Loblolly pine stem wood, residue, and bark. J Agric Food Chem. 2011;59(24):12910–6.

[27] Sluiter A, Hames B, Ruiz R, Scarlata C, Sluiter J, Templeton D, et al. Determination of structural carbohydrates and lignin in biomass. National Renewable Energy Laboratory (NREL) Laboratory Analytical Procedures (LAP) for standard biomass analysis. 2007. NREL/TP-510-42618.

[28] Rajan K, Carrier DJ. Effect of dilute acid pretreatment conditions and washing on the production of inhibitors and on recovery of sugars during wheat straw enzymatic hydrolysis. Biomass Bioenerg. 2014;62:222–7.

[29] Pinto PC, Oliveira C, Costa CA, Gaspar A, Faria T, Ataíde J, et al. Kraft delignification of energy crops in view of pulp production and lignin valorization. Ind Crop Prod. 2015;71:153–62.

[30] Lai YZ, Funaoka M. The distribution of phenolic hydroxyl groups in hardwood lignins. J Wood Chem Technol. 1993;13(1):43–57.

[31] Schwarz P, Youngs V, Shelton D. Isolation and characterization of lignin from hard red spring wheat bran. Cereal Chem. 1989;66(4):289–95.

[32] Lange PW. The distribution of the components in the plant cell wall. Sweden: Stockholm University; 1954.

[33] Seca AM, Cavaleiro JA, Domingues FM, Silvestre AJ, Evtuguin D, Neto CP. Structural characterization of the lignin from the nodes and internodes of *Arundo donax* reed. J Agric Food Chem. 2000;48(3):817–24.

[34] Guerra A, Filpponen I, Lucia LA, Argyropoulos DS. Comparative evaluation of three lignin isolation protocols for various wood species. J Agric Food Chem. 2006;54(26): 9696–705.

[35] You TT, Zhang LM, Zhou SK, Xu F. Structural elucidation of lignin-carbohydrate complex (LCC) preparations and lignin from *Arundo donax* Linn. Ind Crop Prod. 2015;71:65–74.

[36] Yuan TQ, Sun SN, Xu F, Sun RC. Structural characterization of lignin from triploid of Populus tomentosa Carr. J Agric Food Chem. 2011;59(12):6605–15.

[37] El Mansouri NE, Salvado J. Structural characterization of technical lignins for the production of adhesives: application to lignosulfonate, kraft, soda-anthraquinone, organosolv and ethanol process lignins. Ind Crop Prod. 2006;24(1):8–16.

[38] Fergus B, Procter A, Scott J, Goring D. The distribution of lignin in sprucewood as determined by ultraviolet microscopy. Wood Sci Technol. 1969;3(2):117–38.

[39] Lundquist K, Josefsson B, Nyquist G. Analysis of lignin products by fluorescence spectroscopy. Holzforschung-Int J Biol Chem Phys Technol Wood. 1978;32(1):27–32.

[40] Parker C. Photoluminescence of Solutions. Amsterdam: American Elsevier; 1968.

[41] Olmstead J, Gray D. Fluorescence spectroscopy of cellulose, lignin and mechanical pulps: a review. J Pulp Pap Sci. 1997;23(12):J571-J81.

[42] Donaldson LA, Singh AP, Yoshinaga A, Takabe K. Lignin distribution in mild compression wood of Pinus radiata. Can J Botany. 1999;77(1):41–50.

[43] Kutscha N, McOrmond R. The suitability fo using fluorescence microscopy for studying lignification in Balsam Fir. Tech. Bull Life Sci, agr Exp Sta, Univ Maine. 1972;(62):15.

[44] Donaldson L, Hague J, Snell R. Lignin distribution in coppice poplar, linseed and wheat straw. Holzforschung. 2001;55(4):379–85.

[45] Ji Z, Zhang X, Ling Z, Zhou X, Ramaswamy S, Xu F. Visualization of Miscanthus× giganteus cell wall deconstruction subjected to dilute acid pretreatment for enhanced enzymatic digestibility. Biotechnol Biofuels. 2015;8(1):1.

[46] Schulz H, Baranska M. Identification and quantification of valuable plant substances by IR and Raman spectroscopy. Vib Spectrosc. 2007;43(1):13–25.

[47] Popescu CM, Popescu MC, Singurel G, Vasile C, Argyropoulos DS, Willfor S. Spectral characterization of eucalyptus wood. Appl Spectrosc. 2007;61(11):1168–77.

[48] Pandey K. A study of chemical structure of soft and hardwood and wood polymers by FTIR spectroscopy. J Appl Polym Sci. 1999;71(12):1969–75.

[49] Boeriu CG, Bravo D, Gosselink RJA, van Dam JEG. Characterisation of structure-dependent functional properties of lignin with infrared spectroscopy. Ind Crop Prod. 2004;20(2):205–18.

[50] Sen S, Patil S, Argyropoulos DS. Methylation of softwood kraft lignin with dimethyl carbonate. Green Chem. 2015;17(2):1077–87.

[51] Jia S, Cox BJ, Guo X, Zhang ZC, Ekerdt JG. Cleaving the β□ O□ 4 bonds of lignin model compounds in an acidic ionic liquid, 1-H-3-methylimidazolium chloride: an optional strategy for the degradation of lignin. ChemSusChem. 2010;3(9):1078–84.

[52] Hergert HL, Kurth E. The isolation and properties of catechol from white fir bark. J Organic Chem. 1953;18(5):521–9.

[53] Jiao JJ, Zhang Y, Liu CM, Liu J, Wu XQ, Zhang Y. Separation and purification of tricin from an antioxidant product derived from bamboo leaves. J Agric Food Chem. 2007;55(25):10086–92.

[54] Wen JL, Sun ZJ, Sun YC, Sun SN, Xu F, Sun RC. Structural characterization of alkali-extractable lignin fractions from bamboo. J Biobased Mater Bio. 2010;4(4): 408–25.

[55] Sipponen MH, Lapierre C, Mechin V, Baumberger S. Isolation of structurally distinct lignin-carbohydrate fractions from maize stem by sequential alkaline extractions and endoglucanase treatment. Bioresour Technol. 2013;133:522–8.

[56] Chen Y, Fan YM, Gao JM, Li HK. Coloring characteristics of in situ lignin during heat treatment. Wood Sci Technol. 2012;46(1–3):33–40.

[57] Raiskila S, Pulkkinen M, Laakso T, Fagerstedt K, Loija M, Mahlberg R, et al. FTIR spectroscopic prediction of Klason and acid soluble lignin variation in Norway spruce cutting clones. Silva Fennica. 2007;41(2):351.

[58] Faix O. Condensation indices of lignins determined by FTIR-spectroscopy. Eur J Wood Wood Products. 1991;49(9):356.

[59] Seca AM, Cavaleiro JA, Domingues FM, Silvestre AJ, Evtuguin D, Pascoal Neto C. Structural characterization of the bark and core lignins from kenaf (Hibiscus cannabinus). J Agric Food Chem. 1998;46(8):3100–8.

[60] Faix O, Stevanovic-Janezic T, Lundquist K. The lignin of the diffuse porous angiosperm tree Triplochyton scleroxylon K. Schum with low syringyl content. J Wood Chem Technol. 1994;14(2):263–78.

[61] Agarwal UP. An overview of Raman spectroscopy as applied to lignocellulosic materials. In: Advances in lignocellulosics characterization. Argyropoulos, D. S. (Ed.); Atlanta: TAPPI Press; 1999. p. 201–225.

[62] Agarwal UP, Reiner RS, Pandey AK, Ralph SA, Hirth KC, Atalla RH, editors. Raman spectra of lignin model compounds. 59th Appita Annual Conference and Exhibition: Incorporating the 13th ISWFPC (International Symposium on Wood, Fibre and Pulping Chemistry), Auckland, New Zealand, 16–19 May 2005: Proceedings; 2005: Appita Inc.

[63] Agarwal U P, Terashima N. FT-Raman study of dehydrogenation polymer (DHP) lignins. Processing of 12th International Symposium of Wood and Pulping Chemistry. Madison, WI: Department of Forest Ecology and Management, University of Wisconsin, 2003, 3: 123–126.

[64] Agarwal UP, Ralph SA. FT-Raman spectroscopy of wood: identifying contributions of lignin and carbohydrate polymers in the spectrum of black spruce (Picea mariana). Appl Spectrosc. 1997;51(11):1648–55.

[65] Sun L, Varanasi P, Yang F, Loque D, Simmons BA, Singh S. Rapid determination of syringyl: guaiacyl ratios using FT-Raman spectroscopy. Biotechnol Bioeng. 2012;109(3): 647–56.

[66] You TT, Ma JF, Guo SQ, Xu F. Study of alkaline lignin from *Arundo donax* Linn based on FT Raman spectroscopy. Spectroscopy Spectral Anal 2014;8:023.

[67] Larsen KL, Barsberg S. Theoretical and Raman spectroscopic studies of phenolic lignin model monomers. J Phys Chem B. 2010;114(23):8009–21.

[68] Liitiä T, Maunu S, Sipilä J, Hortling B. Application of solid-state 13 C NMR spectroscopy and dipolar dephasing technique to determine the extent of condensation in technical lignins. Solid State Nucl Magn Reson. 2002;21(3):171–86.

[69] Capanema EA, Balakshin MY, Kadla JF. Quantitative characterization of a hardwood milled wood lignin by nuclear magnetic resonance spectroscopy. J Agric Food Chem. 2005;53(25):9639–49.

[70] Pu Y, Cao S, Ragauskas AJ. Application of quantitative 31P NMR in biomass lignin and biofuel precursors characterization. Energ Environ Sci. 2011;4(9):3154–66.

[71] Zhang L, Gellerstedt G. Quantitative 2D HSQC NMR determination of polymer structures by selecting suitable internal standard references. Magn Reson Chem. 2007;45(1):37–45.

[72] Pan XJ, Kadla JF, Ehara K, Gilkes N, Saddler JN. Organosolv ethanol lignin from hybrid poplar as a radical scavenger: relationship between lignin structure, extraction conditions, and antioxidant activity. J Agric Food Chem. 2006;54(16): 5806–13.

[73] Wen JL, Sun SL, Xue BL, Sun RC. Recent advances in characterization of lignin polymer by solution-state nuclear magnetic resonance (NMR) methodology. Materials. 2013;6(1):359–91.

[74] Ralph S, Ralph J, Landucci L, Landucci L. NMR Database of Land Cell Wall Model Compounds. US Forest Prod Lab; Madison, WI (http://ars usda gov/Services/docs htm); 2004.

[75] Lundquist K. NMR studies of lignins. 4. Investigation of spruce lignin by 1H NMR spectroscopy. Acta Chem Scand B. 1980;34:21–6.

[76] Robert D. Carbon-13 nuclear magnetic resonance spectrometry. In: Methods in lignin chemistry. Lin, S. Y., & Dence, C. W. (Eds.); Berlin Heidelberg: Springer; 1992. p. 250–273.

[77] Kringstad KP, Mörck R. 13C-NMR spectra of kraft lignins. Holzforschung-Int J Biol Chem Phys Technol Wood. 1983;37(5):237–44.

[78] Saake B, Argyropoulos DS, Beinhoff O, Faix O. A comparison of lignin polymer models (DHPs) and lignins by 31 P NMR spectroscopy. Phytochemistry. 1996;43(2):499–507.

[79] Faix O, Argyropoulos DS, Robert D, Neirinck V. Determination of hydroxyl groups in lignins evaluation of 1H-, 13C-, 31P-NMR, FTIR and wet chemical methods. Holzforschung-Int J Biol Chem Phys Technol Wood. 1994;48(5):387–94.

[80] Fasching M, Schroder P, Wollboldt RP, Weber HK, Sixta H. A new and facile method for isolation of lignin from wood based on complete wood dissolution. Holzforschung. 2008;62(1):15–23.

[81] Lundquist K. Proton (1H) NMR spectroscopy. In: Methods in lignin chemistry. Lin, S. Y., & Dence, C. W. (Eds.); Berlin Heidelberg: Springer; 1992. 1992. p. 242–249.

[82] Tejado A, Pena C, Labidi J, Echeverria J, Mondragon I. Physico-chemical characterization of lignins from different sources for use in phenol–formaldehyde resin synthesis. Bioresour Technol. 2007;98(8):1655–63.

[83] Rokhin A, Kanitskaya L, Kushnarev D, Kalabin G, Smirnova L, Abduazimov KA, et al. Quantitative1H and13C NMR spectroscopies of cottonplant dioxane lignin. Chem Nat Compd. 1994;30(6):745–53.

[84] Nimz H, Robert D, Faix O, Nemr M. Carbon-13 NMR spectra of lignins, 8. Structural differences between lignins of hardwoods, softwoods, grasses and compression wood. Holzforschung-Int J Biol, Chem, Phys Technol Wood. 1981;35(1):16–26.

[85] Holtman KM, Chang HM, Jameel H, Kadla JF. Quantitative 13C NMR characterization of milled wood lignins isolated by different milling techniques. J Wood Chem Technol. 2006;26(1):21–34.

[86] Akim L, Shevchenko S, Zarubin MY. 13C NMR studies on lignins depolymerized with dry hydrogen iodide. Wood Sci Technol. 1993;27(4):241–8.

[87] Liitiä T. Application of modern NMR spectroscopic techniques to structural studies of wood and pulp components. Finland: University of Helsinki; 2002.

[88] Liitia TM, Maunu SL, Hortling B, Toikka M, Kilpelainen I. Analysis of technical lignins by two- and three-dimensional NMR spectroscopy. J Agric Food Chem. 2003;51(8): 2136–43.

[89] Ede RM, Brunow G. Application of two-dimensional homo-and heteronuclear correlation NMR spectroscopy to wood lignin structure determination. J Organic Chem. 1992;57(5):1477–80.

[90] Kilpelaeinen I, Sipilae J, Brunow G, Lundquist K, Ede RM. Application of two-dimensional NMR spectroscopy to wood lignin structure determination and identification of some minor structural units of hard-and softwood lignins. J Agric Food Chem. 1994;42(12):2790–4.

[91] Sette M, Wechselberger R, Crestini C. Elucidation of lignin structure by quantitative 2D NMR. Chem—Eur J. 2011;17(34):9529–35.

[92] Martínez ÁT, Rencoret J, Marques G, Gutiérrez A, Ibarra D, Jiménez-Barbero J, et al. Monolignol acylation and lignin structure in some nonwoody plants: a 2D NMR study. Phytochemistry. 2008;69(16):2831–43.

[93] Balakshin M, Capanema E, Gracz H, Chang H-m, Jameel H. Quantification of lignin–carbohydrate linkages with high-resolution NMR spectroscopy. Planta. 2011;233(6): 1097–110.

[94] del Río JC, Rencoret J, Marques G, Gutiérrez A, Ibarra D, Santos JI, et al. Highly acylated (acetylated and/or p-coumaroylated) native lignins from diverse herbaceous plants. J Agric Food Chem. 2008;56(20):9525–34.

[95] Ämmälahti E, Brunow G, Bardet M, Robert D, Kilpeläinen I. Identification of side-chain structures in a poplar lignin using three-dimensional HMQC-HOHAHA NMR spectroscopy. J Agric Food Chem. 1998;46(12):5113–7.